

# Size-Selective Hydrogenation of Olefins by Dendrimer-Encapsulated Palladium Nanoparticles

Yanhui Niu, Lee K. Yeung,<sup>†</sup> and Richard M. Crooks<sup>\*‡</sup>

Contribution from the Department of Chemistry, Texas A&M University, P.O. Box 30012, College Station, Texas 77842-3012

Received February 26, 2001

**Abstract:** Nearly monodisperse ( $1.7 \pm 0.2$  nm) palladium nanoparticles were prepared within the interiors of three different generations of hydroxyl-terminated poly(amidoamine) (PAMAM) dendrimers. These dendrimer-encapsulated catalysts (DECs) were used to hydrogenate allyl alcohol and four  $\alpha$ -substituted derivatives in a 4:1 methanol/water mixture. The results indicate that steric crowding on the dendrimer periphery, which increases with dendrimer generation, can act as an adjustable-mesh nanofilter. That is, by controlling the packing density on the dendrimer periphery, it is possible to control access of substrates to the encapsulated catalytic nanoparticle. In general, higher-generation DECs or larger substrates resulted in lower turnover frequencies (although some interesting exceptions were noted). Although the main products of the olefin hydrogenation reactions were the corresponding alkanes, ketones were also obtained when monosubstituted  $\alpha$ -olefins were used as substrates. NMR spectroscopy was used to measure the size selectivity of DECs for the competitive hydrogenation of allyl alcohol and 3-methyl-1-penten-3-ol. The effect on catalytic rate as a function of nanoparticle size is also briefly discussed.

## Introduction

In this paper we show that dendrimer-encapsulated catalysts (DECs), consisting of Pd nanoparticles contained within poly(amidoamine) (PAMAM) dendrimers,<sup>1</sup> are highly selective catalysts for hydrogenation reactions.<sup>2</sup> Specifically, we have examined the catalytic activity of a series of DECs toward hydrogenation of allyl alcohol and four  $\alpha$ -substituted derivatives having different sizes and shapes. The interesting result is that by controlling the steric crowding on the dendrimer periphery it is possible to selectively control access of substrates to the encapsulated metal particle. Because selectivity is induced by the dendrimer, rather than by the intrinsically nonselective Pd catalyst, this approach should be generally applicable to any reaction that involves a catalyst that can be placed within the interior of a dendrimer or related nanoporous materials.

We have previously shown that metal<sup>2–6</sup> and semiconductor<sup>7</sup> nanoparticles of nearly monodisperse size can be prepared within dendritic hosts. These composite materials are easily prepared by mixing together solutions containing dendrimers and metal ions such as Pt<sup>2+</sup>, Pd<sup>2+</sup>, Au<sup>3+</sup>, Cu<sup>2+</sup>, Ni<sup>2+</sup>.<sup>1,8</sup> In favorable cases

the metal ions partition into the dendrimer where they are strongly complexed by interior tertiary amine groups. Subsequent chemical reduction of the dendrimer/metal ion composite yields a zerovalent metal nanoparticle that remains sterically trapped within the dendrimer. Because the dendrimers are nearly monodisperse in size and chemical composition they contain a nearly monodisperse number of interior tertiary amine groups. Because the maximum metal ion/dendrimer ratio is fixed for a particular metal ion, it follows that the maximum number of metal ions sorbed into the dendrimer is also nearly monodisperse and that the resulting nanoparticles are, likewise, of similar size. That is, the nanoparticle replica is a good representation of the dendritic template from which it is prepared.

Dendrimers have been shown to be effective for enabling chemical separations based on the size, shape, and charge of the dendrimer or the species being separated, and they have also been used as stationary phases and additives for various liquid-phase separation methods such as capillary electrophoresis.<sup>9,10</sup> Composite materials having dendrimers incorporated into the structure have also been used to prepare selectively permeable electrode coatings,<sup>11,12</sup> xerogels,<sup>13</sup> and organic membranes for gas separations.<sup>14</sup> All of these separation processes are based on interactions between dendrimers and the much smaller analyte molecules. There are two classes of interactions between dendrimers and smaller molecules: those involving physical interactions, such as size and shape, and those involving electronic interactions, such as surface charge and polarity.

- (9) Gray, A. L.; Hsu, J. T. *J. Chromatogr., A* **1998**, *824*, 119–124.
- (10) Gao, H. Y.; Carlson, J.; Stalcup, A. M.; Heineman, W. R. *J. Chromatogr. Sci.* **1998**, *36*, 146–154.
- (11) Dermody, D. L.; Peez, R. F.; Bergbreiter, D. E.; Crooks, R. M. *Langmuir* **1999**, *15*, 885–890.
- (12) Liu, Y.; Zhao, M.; Bergbreiter, D. E.; Crooks, R. M. *J. Am. Chem. Soc.* **1997**, *119*, 8720–8721.
- (13) Kriesel, J. W.; Tilley, T. D. *Chem. Mater.* **1999**, *11*, 1190–1193.
- (14) Kovvali, A. S.; Chen, H.; Sirkar, K. K. *J. Am. Chem. Soc.* **2000**, *122*, 7594–7595.

\* Author to whom correspondence should be addressed.

<sup>†</sup> Present address: The Dow Chemical Company, Freeport, TX 77541.

<sup>‡</sup> E-mail: crooks@tamu.edu. Telephone: 979-845-5629. Fax: 979-845-1399.

(1) Crooks, R. M.; Zhao, M.; Sun, L.; Chechik, V.; Yeung, L. K. *Acc. Chem. Res.* **2001**, *34*, 181–190.

(2) Zhao, M.; Crooks, R. M. *Angew. Chem., Int. Ed.* **1999**, *38*, 364–366.

(3) Zhao, M.; Sun, L.; Crooks, R. M. *J. Am. Chem. Soc.* **1998**, *120*, 4877.

(4) Zhao, M.; Crooks, R. M. *Adv. Mater.* **1999**, *11*, 217–220.

(5) Yeung, L. K.; Lee, C. T. J.; Johnston, K. P.; Crooks, R. M. *Chem. Commun.* Manuscript submitted.

(6) Yeung, L. K.; Crooks, R. M. *Nano Lett.* **2001**, *1*, 14–17.

(7) Lemon, B. I.; Crooks, R. M. *J. Am. Chem. Soc.* **2000**, *122*, 12886–12887.

(8) Grohn, F.; Bauer, B. J.; Akpalu, Y. A.; Jackson, C. L.; Amis, E. J. *Macromolecules* **2000**, *33*, 6042–6050.




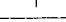


While it not possible to fully separate these factors, Meijer et al. demonstrated that dendrimers could selectively encapsulate analyte molecules based on shape.<sup>15,16</sup> Similarly, we have shown that by controlling the pH of a solution dendrimers can act as molecular-gates, admitting molecules on the basis of overall charge.<sup>2,11,12</sup>

The selective nature of dendrimers can also be applied to problems in catalysis. Specifically, we envision that dendrimers encapsulating catalysts may act as selective gates that control the access of small molecules to the embedded catalytic moiety. In this regard, it is productive to think of the dendrimer as a nanofilter having a mesh that can be controlled by chemically altering the periphery. Indeed, others have previously recognized that dendritic structures have the potential to function as selective moieties in catalytic processes. For example, dendrons grafted onto metalloporphyrins were shown to be selective for different-shaped ligands<sup>17</sup> as well as for epoxidation substrates.<sup>18,19</sup> Dendrimers containing metal ion cores and dendritic ligands have also been shown to affect both selectivity and reactivity for Ru(II)-catalyzed asymmetric hydrogenations<sup>20</sup> and Cu(II)-catalyzed Diels–Alder reactions.<sup>21</sup> These catalysts were composed of a catalytically active species surrounded by a dendritic shell designed to regulate both substrate selectivity and overall catalytic reactivity.

There are two characteristics of DEC catalysts that make them particularly attractive for catalysis. First, solubility is controlled principally by the chemical composition of the dendrimer periphery.<sup>1</sup> Second, because the encapsulated particles are very small (typically 1–3 nm),<sup>1</sup> they have a high surface-area-to-volume ratio, which is important for high efficiency.<sup>22,23</sup> We have taken advantage of these properties to show that DEC catalysts are effective for the reduction of olefins in aqueous,<sup>2,4</sup> organic,<sup>24</sup> and fluorinated<sup>25</sup> solvents. Additionally, synthetically more useful carbon–carbon bond-forming reactions have been catalyzed by Pd(0) nanoparticles encapsulated in modified poly(propylene imine) (PPI) dendrimers in both hydrocarbon/fluorocarbon<sup>6</sup> and supercritical CO<sub>2</sub> solvent<sup>5</sup> systems.

Although some data in our previous reports suggested high levels of selectivity for either a particular substrate or a particular product,<sup>1</sup> no detailed study correlating dendrimer size and structure to a catalytic process has thus far been reported. Accordingly, this report is the first quantitative study correlating DEC structure to catalytic rate. Specifically, the catalytic efficiency of dendrimer encapsulated Pd nanoparticles toward reduction of the double bond in differently shaped allylic alcohols (Table 1, 1–5) is reported. Three generations of PAMAM dendrimers were used as the template, while the size of the catalytic nanoparticle was kept constant by controlling the amount of Pd(II) salt used for the DEC synthesis. The results

**Table 1.** Hydrogenation Reaction Rates Using GnOH/Pd(0)40 Catalysts for Structurally Related Allylic Alcohols<sup>a</sup>

Substrates	TOF [mol H <sub>2</sub> (mol Pd) <sup>-1</sup> h <sup>-1</sup> ]		
	G4OH/Pd(0)40	G6OH/Pd(0)40	G8OH/Pd(0)40
(1) 	480/470 <sup>2</sup>	450/460 <sup>2</sup>	120
(1) 	220 <sup>1</sup>	200 <sup>1</sup>	130 <sup>1</sup>
(2) 	450/460 <sup>2</sup>	380	93
(3) 	260	280	68
(4) 	150	75	62
(5) 	100	40	50

<sup>a</sup> Hydrogenation reactions were carried out at 25 ± 2 °C with 2 × 10<sup>-4</sup> M Pd(0) composite catalysts in MeOH–H<sub>2</sub>O (4:1 v/v) mixtures. The turnover frequency (TOF) was calculated on the basis of H<sub>2</sub> uptake (mol of H<sub>2</sub> per mol of Pd(0) per h). <sup>1</sup> Hydrogenation reactions were carried out at 25 ± 2 °C with 2 × 10<sup>-4</sup> M Pd(0) composite catalysts in H<sub>2</sub>O only (no methanol). <sup>2</sup> Duplicate measurements were performed to illustrate the level of run-to-run reproducibility.

indicate that the activity of DEC catalysts for a particular substrate can be controlled by varying the generation of the dendrimer and that for a particular DEC turnover frequencies (TOFs) differ significantly depending on the size and shape of the substrate.

## Experimental Section

**Materials.** Hydroxyl-terminated fourth-, sixth-, and eighth-generation (G4OH, G6OH, and G8OH, respectively) poly(amidoamine) (PAMAM) dendrimers having an ethylenediamine core were obtained as 10–25% methanol solutions (Dendritech, Inc., Midland, MI). Prior to use, the methanol was removed under vacuum at room temperature. The unsaturated alcohols, methanol, deuterated solvents, and NaBH<sub>4</sub> were used as received from the Aldrich Chemical Co. (Milwaukee, WI). K<sub>2</sub>-PdCl<sub>4</sub> was purchased from Strem Chemicals, Inc. (Newburyport, MA) and used without further purification. 18 MΩ-cm Milli-Q water (Millipore, Bedford, MA) was used to prepare aqueous solutions. Cellulose dialysis sacks having a molecular weight cutoff of 12 000 were purchased from Sigma Diagnostics, Inc. (St. Louis, MO).

**Instrumentation.** <sup>1</sup>H and <sup>13</sup>C NMR spectra were recorded on a Unity p300 spectrometer at 300 MHz (75 MHz for <sup>13</sup>C). High-resolution transmission electron micrographs (HRTEM) were obtained with a JEOL-2010 transmission electron microscope having a point-to-point resolution of 0.19 nm. Samples were prepared by placing a drop of solution on a holey-carbon-coated Cu TEM grid and allowing the solvent to evaporate in air. GC data were recorded on a HP 5890 GC system, equipped with J&W DB-FFAP columns (30 m length, 0.32 mm i.d., 0.25 μm film, column head pressure 14 psi) and a flame ionization detector. Helium was used as the carrier gas. The initial temperature was set at 32 °C and increased at a rate of 10 °C/min.

**Preparation of GnOH/Pd(0) Catalysts.** A 5 × 10<sup>-3</sup> M aqueous solution of GnOH (n = 4, 6, 8) PAMAM dendrimer was prepared from dry GnOH. The GnOH/Pd(II) complex was prepared by adding 50 μL of the GnOH solution into 9.75 mL of purified water, followed by 100 μL of a 0.1 M K<sub>2</sub>PdCl<sub>4</sub> (aq) solution (40 eq) under vigorous stirring. A light yellow solution was obtained immediately. After stirring for 30 min, 100 μL of a 1 M NaBH<sub>4</sub> (aq) solution was added, which changed the color of the solution to golden brown. The solution was purified by overnight dialysis against water. Then 40 mL of methanol was added to the solution to prepare the catalytic solution.

**Hydrogenation Apparatus.** Hydrogenation reactions were carried out in a 150 mL round-bottomed Schlenk flask with an adapter connected to the top of a buret filled with hydrogen gas. A three-way stopcock was used with one arm attached to a hydrogen gas cylinder, the second to the gas buret, and the third to the reaction flask. A dibutyl phthalate-filled reservoir was connected to the bottom of the buret and

(15) Jansen, J. F. G. A.; de Brabander-van den Berg, E. M. M.; Meijer, E. W. *Science* **1994**, *266*, 1226–1229.

(16) Jansen, J. F. G. A.; de Brabander-van den Berg, E. M. M.; Meijer, E. W. *J. Am. Chem. Soc.* **1995**, *117*, 4417–4418.

(17) Bhyrappa, P.; Vajjayanthimala, G.; Suslick, K. S. *J. Am. Chem. Soc.* **1999**, *121*, 262–263.

(18) Bhyrappa, P.; Young, J. K.; Moore, J. S.; Suslick, K. S. *J. Am. Chem. Soc.* **1996**, *118*, 5708–5711.

(19) Bhyrappa, P.; Young, J. K.; Moore, J. S.; Suslick, K. S. *J. Mol. Catal., A* **1996**, *113*, 109–116.

(20) Fan, Q. H.; Chen, Y. M.; Chen, X. M.; Jiang, D. Z.; Xi, F.; Chan, A. S. C. *Chem. Commun.* **2000**, *9*, 789–790.

(21) Chow, H. F.; Mak, C. C. *J. Org. Chem.* **1997**, *62*, 5116–5127.

(22) Lewis, L. N. *Chem. Rev.* **1993**, *93*, 2693–2730.

(23) Hirai, H. *J. Macromol. Sci., Chem.* **1979**, *A13*, 633–649.

(24) Chechik, V.; Zhao, M.; Crooks, R. M. *J. Am. Chem. Soc.* **1999**, *121*, 4910–4911.

(25) Chechik, V.; Crooks, R. M. *J. Am. Chem. Soc.* **2000**, *122*, 1243–1244.

open to the atmosphere at the top. All of the hydrogenation reactions were run at atmospheric pressure and room temperature ( $25 \pm 2$  °C).

**Hydrogenation Reactions.** 50 mL of the catalytic solution and a magnetic stir bar were placed in a Schlenk flask. All of the joints of the apparatus were sealed with silicone grease and checked for leaks before adding the substrate. The system was purged with  $H_2$  for 15 min. To verify that  $H_2$  was not consumed in the absence of substrate, the catalyst was stirred in solution over a known volume of  $H_2$ . The  $H_2$  volume did not change over a period of hours. Experiments were carried out by adding 10 mmol of substrate by syringe under vigorous stirring conditions. The rate of stirring was maintained high and constant throughout all hydrogenation reactions. There was no evidence for Pd(0) aggregation during or after hydrogenation of the substrates in the MeOH– $H_2O$  solvent system, indicating that the catalysts are stable on the time scale of the reactions.

**NMR Characterization of Hydrogenation Reaction Products.** The products of the hydrogenation reactions were identified by  $^1H$  NMR by performing the catalytic reactions in deuterated solvents. When more than one product was observed,  $^{13}C$  NMR spectra were also obtained. The procedure was the same for all substrates and is illustrated using allyl alcohol as an example. Ten microliters of a  $5 \times 10^{-4}$  M G4OH aqueous solution was added to 170  $\mu L$  of  $D_2O$  in a reaction vial, followed by 2  $\mu L$  of 0.1 M  $K_2PdCl_4$  (0.2  $\mu mol$ ) under vigorous stirring for 30 min. Then 1 mg of  $NaBH_4$  (26  $\mu mol$ ) was added with stirring. After 30 min, 682  $\mu L$  of  $CD_3OD$  was added ( $CD_3OD/D_2O = 4$ ) to aid in solubilizing the substrate, and then 136  $\mu L$  of allyl alcohol (2.0 mmol) was added. A  $^1H$  NMR spectrum of this solution was obtained just prior to the hydrogenation reaction. The hydrogenation reaction was then performed in a reaction vial using the previously described apparatus. After 24 h the reaction mixture was analyzed by  $^1H$  NMR to identify the reaction product(s) (48 h after hydrogenation of substrates 4 and 5).

***n*-Propanol (1a):**  $^1H$  NMR:  $\delta$  1.06 (t,  $CH_3$ , 3H), 1.69 (m,  $CH_2$ , 2H), 3.66 (t,  $CH_2$ , 2H), 4.81 (b, OH, 1H).

**2-Butanol (2a) and ethyl methyl ether (2b) mixture:**  $^1H$  NMR:  $\delta$  0.90 (t,  $CH_3$ , 3H), 1.01 (t,  $CH_3$ , 3H), 1.14 (d,  $CH_3$ , 3H), 1.45 (m,  $CH_2$ , 2H), 2.16 (s,  $CH_3$ , 3H), 2.53 (q,  $CH_2$ , 2H), 3.66 (m, CH, 1H), 4.86 (b, OH, 1H);  $^{13}C$  NMR:  $\delta$  8.56, 10.56, 22.97, 29.76, 32.72, 37.64, 70.13, 214.70.

**3-Pentanol (3a) and diethyl ether (3b) mixture:**  $^1H$  NMR:  $\delta$  0.92 (t,  $CH_3$ , 6H), 1.02 (t,  $CH_3$ , 3H), 1.45 (m,  $CH_2$ , 4H), 2.49 (q,  $CH_2$ , 4H), 3.39 (m, CH, 1H), 4.63 (b, OH, 1H);  $^{13}C$  NMR:  $\delta$  8.44, 10.56, 30.36, 36.32, 75.36, 216.55.

**2-Methyl-2-butanol (4a):**  $^1H$  NMR:  $\delta$  0.90 (t,  $CH_3$ , 3H), 1.17 (s,  $CH_3$ , 6H), 1.49 (q,  $CH_2$ , 2H), 4.65 (b, OH, 1H).

**3-Methyl-3-pentanol (5a):**  $^1H$  NMR:  $\delta$  0.88 (t,  $CH_3$ , 6H), 1.10 (s,  $CH_3$ , 3H), 1.47 (q,  $CH_2$ , 4H), 4.76 (b, OH, 1H).

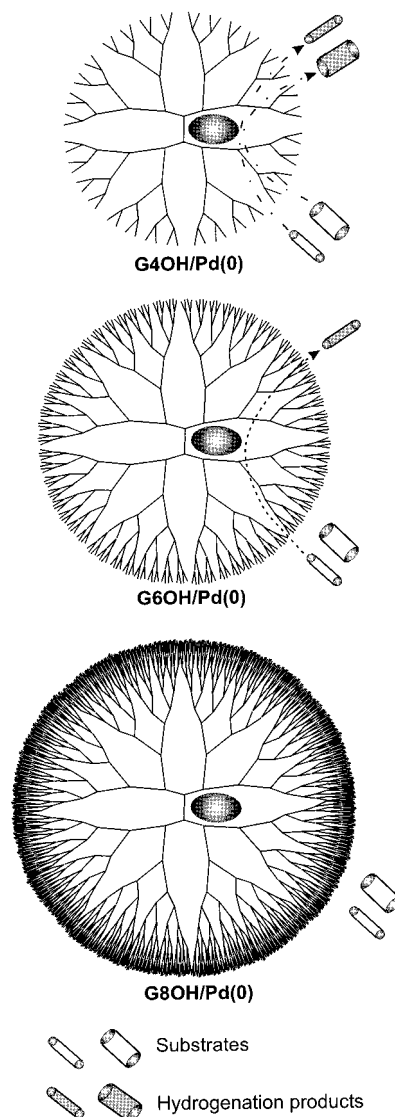
**NMR Study of G4OH Substrate Selectivity.** Ten microliters of a  $5 \times 10^{-4}$  M aqueous solution of G4OH was added to 149  $\mu L$  of  $D_2O$  in a reaction vial followed by 4  $\mu L$  of 0.05 M  $K_2PdCl_4$  (0.2  $\mu mol$ ) under vigorous stirring for 30 min. One milligram of  $NaBH_4$  (26  $\mu mol$ ) was then added with stirring. After 30 min, 650  $\mu L$   $CD_3OD$  was added ( $CD_3OD/D_2O = 4$ ) followed by 68  $\mu L$  of allyl alcohol (**1**) (1.0 mmol) and 120  $\mu L$  of 3-methyl-1-penten-3-ol (**5**) (1.0 mmol). A  $^1H$  NMR spectrum of this reaction mixture was obtained just prior to the treatment with hydrogen. The hydrogenation reaction was then carried out using the previously described apparatus.  $^1H$  NMR spectra were obtained after 2.5, 5.0, 20, and 42 h to determine the product distribution.

**Molecular Modeling.** Molecular models were created using the Cerius<sup>2</sup> (version 4.0) software package (Molecular Simulations, Inc., San Diego, CA). The free volume and dimensions of the substrates (**1–5**) were measured on the basis of their optimized structures obtained using MOPAC calculations.

## Results and Discussion

We previously showed that hydroxyl-terminated PAMAM dendrimers (GnOH) can be used as templates for the encapsulation of Pd(0) and Pt(0) nanoparticles in aqueous solution.<sup>2,4</sup> The size of the entrapped metal nanoparticles can be controlled either by using different dendrimer generations or manipulating the

**Scheme 1**



dendrimer/metal-ion ratio.<sup>2–4</sup> For the present study, we are interested in probing the extent of substrate selectivity imparted to the DEC by the surrounding dendrimer “nanofilter”. The hypothesis is that dendrimer generation can be used to select substrates based on their size, because higher generation dendrimers have more crowded surfaces which limit access of the substrate to the encapsulated nanoparticle (Scheme 1). To test this hypothesis, we prepared dendrimer-encapsulated nanoparticles containing an average of 40 Pd atoms within the interior of GnOH dendrimers ( $n = 4, 6, 8$ , where  $n$  corresponds to different PAMAM generations). This results in a homologous series of DECs in which only the porosity of the dendrimer and their diameter vary. The hydrogenation rates of chemically similar, but structurally different, olefins were then measured to test the aforementioned hypothesis. A decrease in turnover frequency (TOF) is anticipated as the substrate size increases (Scheme 1).

Because allyl alcohol (**1**) is the simplest unsaturated alcohol and was used as a substrate in a prior study,<sup>2</sup> it was a natural starting point for this work. The following structurally related materials were also studied: 3-buten-2-ol (**2**), 1-penten-3-ol (**3**), 2-methyl-3-buten-2-ol (**4**), and 3-methyl-1-penten-3-ol (**5**) (the structures of all five substrates are provided in Table 1). Importantly, it has been shown previously that the intrinsic TOFs

of C3–C6 unsaturated alcohols, which are structurally similar to the allylic alcohols used here, differ only slightly.<sup>26</sup> Accordingly, it is appropriate to ascribe the differences in TOFs discussed later to dendrimer-induced size selectivity rather than to intrinsic properties of the substrates. Because the solubility of substituted alcohols in H<sub>2</sub>O is not as great as in MeOH, a MeOH–H<sub>2</sub>O (4:1, v/v) mixed solvent system was chosen to maintain a homogeneous reaction mixture.

The composite catalysts used in this study are composed of Pd(0) nanoclusters encapsulated within G4OH, G6OH, and G8OH PAMAM dendrimers. In each case the DEC was prepared using a Pd(II)-to-dendrimer ratio of 40. We expected, and transmission electron microscopy confirmed, that following reduction the average Pd(0) cluster size was independent of dendrimer generation. Specifically, the encapsulated Pd(0) nanoparticles had an average diameter and dispersity of  $1.7 \pm 0.2$  nm regardless of the dendrimer generation (see Supporting Information).

The rate of hydrogenation for the five allylic alcohol substrates (1–5) in the presence of the three catalysts was determined by H<sub>2</sub> uptake (Table 1). Turnover frequencies (TOFs, mol of H<sub>2</sub> per mol of Pd(0) per h) in the mixed solvent ranges from 40 to 480 depending on the dendrimer generation and substrate. Qualitatively, Table 1 indicates that for a particular catalyst (dendrimer generation) the TOFs generally decrease as the substrates become bulkier. For example, the maximum TOF for the G4OH/Pd(0)40 catalyst for the hydrogenation of allyl alcohol (1) was 480 mol H<sub>2</sub>(mol Pd)<sup>-1</sup> h<sup>-1</sup>. This reaction rate is comparable to that obtained using polymer-supported Pd(0) catalysts in methanol (565 mol H<sub>2</sub>(mol Pd)<sup>-1</sup> h<sup>-1</sup>)<sup>27</sup> and PAMAM encapsulated Pd(0) in fluoros-phase solvent (400 mol H<sub>2</sub>(mol Pd)<sup>-1</sup> h<sup>-1</sup>).<sup>25</sup> A substrate having one  $\alpha$  methyl group, 3-buten-2-ol (2), yielded a slightly lower TOF. When the methyl group was changed to ethyl (3), the reaction rate decreased further to 260 mol H<sub>2</sub>(mol Pd)<sup>-1</sup> h<sup>-1</sup>. This trend continues when two methyl groups are present at the  $\alpha$  position (4) and when both a methyl and an ethyl group are present at the  $\alpha$  position of the substrate (5). Overall, the TOF for the bulkiest substrate (5) was nearly 5 times lower than the smallest (1). The same trend was found for the G6OH/Pd(0)40 and G8OH/Pd(0)40 catalysts.

It is possible to correlate these experimental data to a semiquantitative structural model of the dendrimer and in particular to the average distance between functional groups on the periphery of the dendrimer. That is, if we make the following five assumptions, then the distance between adjacent terminal groups for the different generation dendrimers can be calculated using appropriate molecular models (see Experimental Section): (1) the dendrimers are spheroidal in shape;<sup>28</sup> (2) all of the terminal groups are located at the surface of the dendrimer;<sup>28,29</sup> (3) the terminal C–O bonds are perpendicular to the dendrimer surface with equal distances among adjacent oxygen atoms; (4) the diameters of the G4OH, G6OH, and G8OH dendrimers are 4.5, 6.7, and 9.7 nm, respectively;<sup>30</sup> and (5) the number of terminal hydroxyl groups for G4OH, G6OH, and G8OH are 64, 256, and 1024, respectively. Using these assumptions, the calculated average edge-to-edge distance

between two O–H end groups (based on the van der Waals surface of the outermost O atoms) in G4OH is 8.2 Å, while the distance decreases to 5.4 Å for G6OH, and further to 3.2 Å for G8OH. These data confirm that the “mesh size” of the dendrimer “nanofilter” depends very sensitively on generation.

Molecular modeling was also used to calculate the free volumes of the five substrates, which are as follows: (1) 60.7, (2) 75.4, (3) 96.1, (4) 89.7, and (5) 103 Å<sup>3</sup>. It seems reasonable that the substrates first penetrate into the dendrimer through their hydroxyl groups, and therefore a good measure of substrate size is the largest linear dimension perpendicular to the O–H bond direction of the allylic alcohols. For substrates 1–5, these values are 5.5, 7.0, 7.5, 7.0, and 8.0 Å, respectively. The results of the molecular modeling parameters (substrate size and dendrimer pore size) correlate well to the experimental data for all three dendrimer generations (Table 1), except for substrate 4, which is smaller than 3 and has a smaller TOF. This suggests that the model described by Scheme 1, which is based solely on stationary steric considerations, is fairly good but does not predict all of the experimental data correctly. Apparently there are chemical and more complex structural aspects of the substrate that must be taken into account to fully resolve this issue, and therefore additional experiments are underway to further refine the model proposed here.

It is interesting to compare hydrogenation rates for the same substrate when different generation dendrimers encapsulate the Pd(0) nanoparticle. Table 1 shows that there is a clear trend in this regard: the lower generation DEC, with just two exceptions, result in the highest TOFs. In addition, for substrates 1–3 there is a much larger decrease in TOF when the generation changes from G6 to G8 than for the change between G4 and G6. These observations correlate well with the average distance between terminal groups of the dendrimers (vide supra: G4OH, 8.2 Å; G6OH, 5.4 Å; G8OH, 3.2 Å). That is, when the dendrimer generation increases to 8, the average distance between terminal groups (3.2 Å) is significantly less than the critical dimension of the substrates (range: 5.5–8.0 Å, vide supra). Thus, because the dendrimer porosity can be controlled by varying either the generation, as in this study, or the bulkiness of the peripheral functional groups, it is possible to prepare selective catalysts using as a first approximation the very simple concept of steric crowding on the dendrimer surface.

We previously reported TOF values for 1 in water only (Table 1),<sup>2</sup> and these rates are generally smaller than in the mixed MeOH–H<sub>2</sub>O solvent used here. Unfortunately, it was not possible to perform a thorough comparison of the reaction rates of all five substrates in both solvent systems due to the limited solubility of most of the substrates and products in pure water. However, allyl alcohol (1) and its hydrogenation product are both appreciably soluble in H<sub>2</sub>O. The TOFs of G4OH/Pd(0)40, G6OH/Pd(0)40, and G8OH/Pd(0)40 for the hydrogenation of allyl alcohol in water are 220, 200, and 130 mol H<sub>2</sub>(mol Pd)<sup>-1</sup> h<sup>-1</sup>, respectively. In contrast, we found the maximum TOFs for allyl alcohol hydrogenation in the mixed MeOH–H<sub>2</sub>O solvent to be greater by about a factor of 2 for G4OH/Pd(0)40 and G6OH/Pd(0)40, but nearly the same for G8OH/Pd(0)40. This result is consistent with previous findings that solvent plays an important role in determining hydrogenation reaction rate at colloidal nanoparticles.<sup>31,32</sup> For example, the hydrogenation of the ethyl ester of mandelic acid in ethanol is much faster than

(26) Kacer, P.; Novak, P.; Cerveny, L. *Collect. Czech. Chem. Commun.* **2000**, *65*, 9–16.

(27) Selvaraj, P. C.; Mahadevan, V. J. *Polym. Sci., Part A: Polym. Chem.* **1997**, *35*, 105–122.

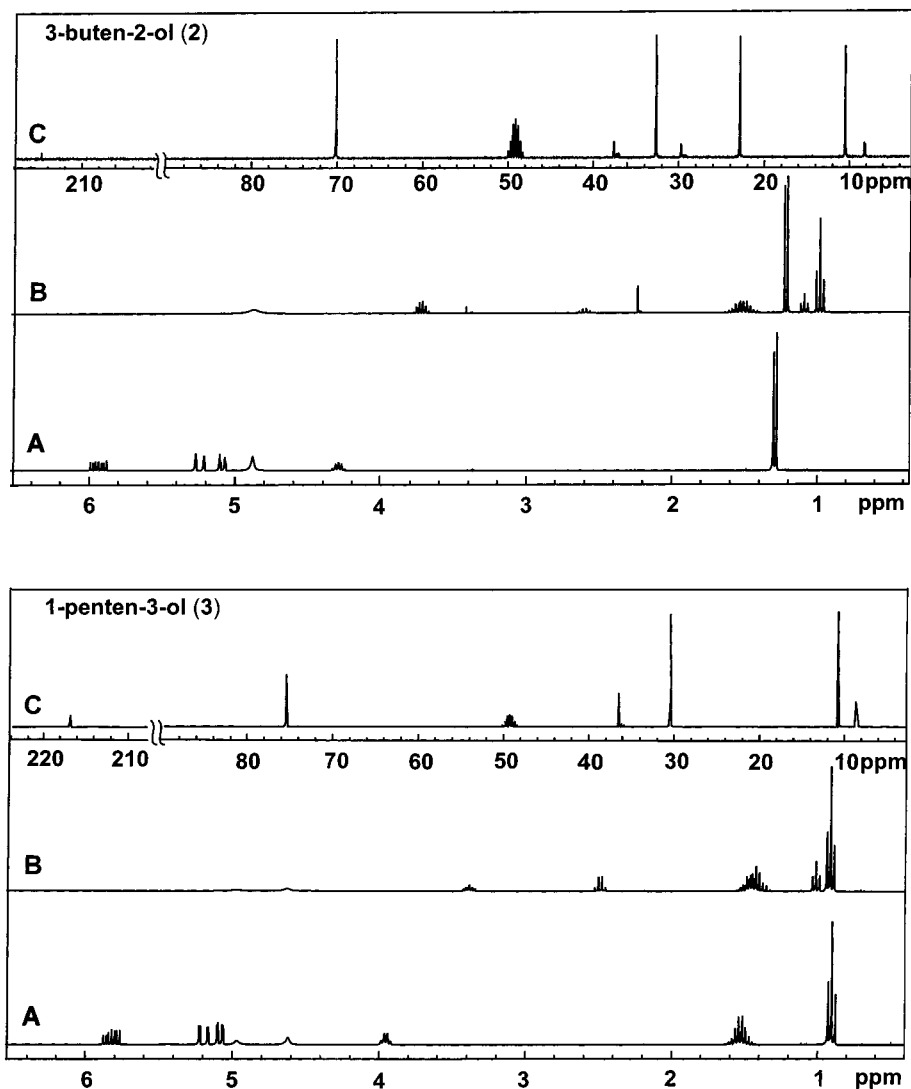
(28) Tomalia, D. A.; Naylor, A. M.; III, W. A. G. *Angew. Chem., Int. Ed. Engl.* **1990**, *29*, 138–175.

(29) Topp, A.; Bauer, B. J.; Klimash, J. W.; Spindler, R.; Tomalia, D. A.; Amis, E. J. *Macromolecules* **1999**, *32*, 7226–7231.

(30) Information provided by Dendritech, Inc.; Midland, MI.

(31) Augustine, R. L.; Warner, R. W.; Melnick, M. J. *J. Org. Chem.* **1984**, *49*, 4853–4856.

(32) Sulman, E.; Bodrova, Y.; Matveeva, V.; Semagina, N.; Cerveny, L.; Kurtc, V.; Bronstein, L.; Platonova, O.; Valetsky, P. *Appl. Catal., A* **1999**, *176*, 75–81.



**Figure 1.**  $^1\text{H}$  NMR spectra of reaction mixtures containing  $5 \times 10^{-6}$  M G4OH/Pd(0)40 and 2 M unsaturated 3-buten-2-ol (**2**) or 1-penten-3-ol (**3**) before (A) and after (B) reaction with  $\text{H}_2$  in  $\text{CD}_3\text{OD}-\text{D}_2\text{O}$  (4:1 v/v). The data shown in parts C are the  $^{13}\text{C}$  NMR spectra of the reaction mixture after hydrogenation.

in water.<sup>33</sup> Other studies have shown that trace amounts of water are very beneficial for increasing the hydrogenation rate in ketonic solvent<sup>34</sup> or methyl acetate.<sup>35</sup> At this time we do not fully understand why there are such large changes in TOF as a function of solvent for nominally identical dendrimer-encapsulated catalysts, but it seems likely that this finding results from changes in the surface chemistry of the encapsulated Pd nanoparticles, structural changes of the dendrimer template driven by differences in solvent polarity, or enhanced partitioning of the substrate into the dendrimer in the mixed solvent.<sup>36,37</sup>

The size of dendrimer-encapsulated nanoparticles can also be used to tune the rate of chemical reactions. Specifically, preliminary results indicate that increasing the size of a Pd nanoparticle leads to a rate enhancement for the hydrogenation reaction. For example, it is possible to hold the ratio of Pd(0) to tertiary amines constant for all three generations of dendrim-

ers. That is, encapsulated Pd(0) clusters containing 40, 164, and 659 atoms can be prepared within G4OH, G6OH, and G8OH, respectively. The allyl alcohol hydrogenation reaction rates measured for the DECs containing large metal particles were extremely fast compared with the data presented thus far: 1000 and 2500 mol  $\text{H}_2$ /(mol Pd) $^{-1}$  h $^{-1}$  TOF for G6OH/Pd(0)164 and G8OH/Pd(0)659, respectively. Interestingly, these larger catalytic particles are not very stable. There are many possible explanations for these findings. For example, metal nanoparticles in this size regime are known to exhibit size-dependent electronic properties that can affect TOFs. Alternatively, mass-transfer effects may be relevant: larger metal particles may be more accessible to substrates than smaller particles when they are encapsulated within the same generation dendrimer. Hypotheses such as these provide a means for refining the simple model shown in Scheme 1.

The hydrogenation products were identified by NMR spectroscopy. The NMR spectra of reaction mixtures of  $5 \times 10^{-6}$  M G4OH/Pd(0)40 and 2.0 M unsaturated alcohols in  $\text{CD}_3\text{OD}-\text{D}_2\text{O}$  (4:1, v/v) before and after treatment with  $\text{H}_2$  are shown in Figure 1 and in the Supporting Information. The reaction products for all five hydrogenation reactions are given in Scheme 2. Characterization of the reaction mixtures is simplified because

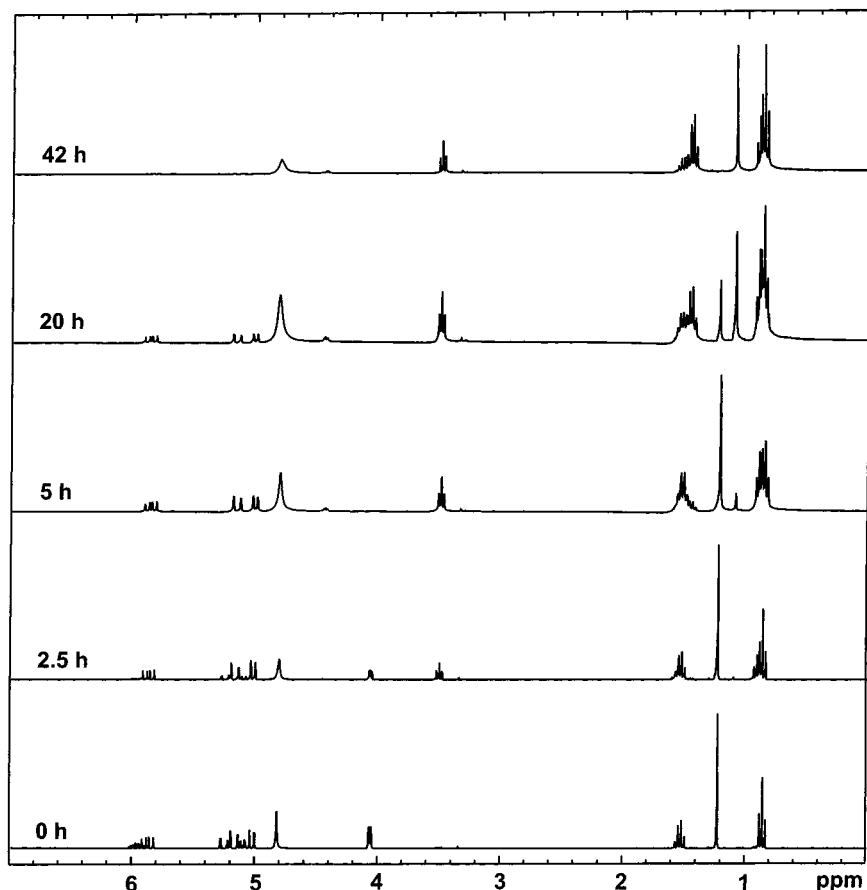
(33) Ronchina, L.; Toniolo, L.; Cavinato, G. *Appl. Catal., A* **1997**, *165*, 133–145.

(34) Collier, P. J.; Iggo, J. A.; Whyman, R. *J. Mol. Catal. A: Chem.* **1999**, *146*, 149–157.

(35) Augustine, R. L.; Tanielyan, S. K.; Doyle, L. K. *Tetrahedron: Asymmetry* **1993**, *4*, 1803–1827.

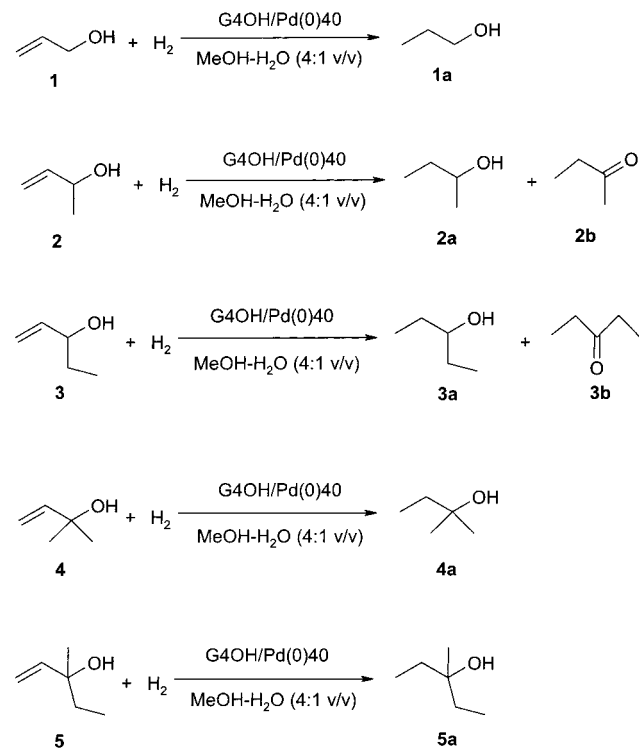
(36) Chai, M.; Niu, Y.; Youngs, W. J.; Rinaldi, P. L. *J. Am. Chem. Soc.* **2001**, ASAP.

(37) Murat, M.; Grest, G. S. *Macromolecules* **1996**, *29*, 1278–1285.



**Figure 2.**  $^1\text{H}$  NMR spectra of a reaction mixture containing  $5 \times 10^{-6}$  M G4OH/Pd(0)40, 1 M allyl alcohol (**1**), and 1 M 3-methyl-1-penten-3-ol (**5**), before reaction with  $\text{H}_2$  and at various time increments after the hydrogenation reaction commenced (solvent:  $\text{CD}_3\text{OD}-\text{D}_2\text{O}$ , 4:1 v/v).

### Scheme 2



the concentration of G4OH/Pd(0) catalyst is below the NMR detection limit. Before the start of each reaction, the spectra of the reaction mixtures showed the characteristic peaks of the vinylic protons (5–6 ppm). After exposure to  $\text{H}_2$ , the dis-

appearance of the double bond peaks indicated that the reaction went to completion. Substrates **1**, **4**, and **5** were cleanly hydrogenated, yielding only the saturated alkyl alcohols without isomerization or any other byproducts (see Supporting Information).

Hydrogenation of substrates **2** and **3**, both of which contain an  $\alpha$  hydrogen, generated not only the anticipated hydrogenation products but also a small amount of byproducts (Scheme 2 and Figure 1). In the case of 1-penten-3-ol (**3**), in addition to the expected product (3-pentanol, **3a**), which has peaks at 3.39 ppm (m), 1.45 ppm (m) and 0.92 ppm (t) in the  $^1\text{H}$  NMR spectrum, there are two extra sets of peaks at 2.49 ppm (q) and 1.02 ppm (t) that correspond to 3-pentanone (**3b**). The characteristic chemical shift at 216.55 ppm in the  $^{13}\text{C}$  NMR spectrum further confirmed the presence of ketone. Integration of the  $^1\text{H}$  NMR spectrum indicated that the ratio of the expected 3-pentanol (**3a**) to the ketone byproduct is 4.7:1. Similarly, hydrogenation of 3-buten-2-ol (**2**) yielded the anticipated alcohol (**2a**) and 2-butanone (**2b**) as a byproduct in a 6.7:1 ratio. GC measurements for both reaction mixtures were made to confirm the NMR data. The formation of byproduct ketones from **2** and **3** is known to involve a double bond migration resulting in the corresponding enol isomers, which then slowly tautomerize to ketones.<sup>38</sup> The important point is that reactions occurring *within* DEC s do not always yield the expected products. Once understood, this finding is likely to be of great value in designing product-selective DEC s.

Having characterized the catalytic properties of the DEC s in single-substrate solvents, we endeavored to demonstrate their

(38) Bergens, S. H.; Bosnich, B. *J. Am. Chem. Soc.* **1991**, *113*, 958–967.

selective nature by performing a competitive hydrogenation reaction. Allyl alcohol (**1**) and 3-methyl-1-penten-3-ol (**5**) were used for this study because the reaction does not yield byproducts and because they have very different TOFs (Table 1). Because **1** is a more linear molecule than **5**, we expected that it would have an easier time navigating through the dendrimer branches than **5**. <sup>1</sup>H NMR spectra of the reaction mixture of **1** and **5** (1:1 mol equiv) before and after treatment with H<sub>2</sub> were recorded as a function of time using G4OH/Pd(0)40 as the catalyst (Figure 2). After 2.5 h of hydrogenation, 50% of the allyl alcohol (**1**) was reduced to *n*-propanol (**1a**), while only 1.6% 3-methyl-3-pentanol (**5a**) was generated. After an additional 2.5 h, 100% of **1** is converted to **1a**, but only 11% **5** was converted to **5a**. After a total reaction time of 20 h, a third of the 3-methyl-1-penten-3-ol was still unconverted to product, but the conversion was finally complete after 42 h. These results correlate well to the single-substrate data in Table 1, and they provide additional support for the model embodied by Scheme 1.

### Summary and Conclusions

In this study we have described a general approach for rendering intrinsically unselective catalysts selective. This strategy involves encapsulation of the nonselective catalyst (the Pd nanoparticle) within a selective nanoporous cage (the dendrimer). As we have shown, these nanoreactors can distinguish between two substrates that differ only slightly in chemical structure. On the basis of the experimental data and molecular modeling results, we have proposed a model (Scheme 1) that attributes selectivity principally to steric interactions between the substrates and the functional groups on the dendrimer periphery. Yet to be examined thoroughly are the effects of different solvents and peripheral groups on reaction rates; those issues are being addressed at the present time and will be reported in due course. The important point, however, is that by simply changing dendrimer generation reaction rates can be varied by nearly a factor of 5 in favorable cases.

Other issues that merit investigation include the effect of the *intradendrimer* reaction medium on product yields. Specifically, is it possible to develop a reasonable model to correlate the interior structure of the dendrimer (which is undoubtedly a strong function of solvent) to product distribution and subsequently design DEC's that are both substrate- and product-selective? Finally, we reported a few tantalizing initial results that correlate TOF to nanoparticle size. Heterogeneous catalysis studies have previously shown that either quantum electronic or structural effects can have a dramatic influence on reaction rates.<sup>39</sup> DEC's are ideally suited for studying such effects for dispersed catalysts.

**Acknowledgment.** We gratefully acknowledge the Office of Naval Research and the Robert A. Welch Foundation for supporting the research. We also thank Dr. Li Sun and Dr. Julio Alvarez for valuable discussions, and Mr. Xu Li for performing the GC measurements and helpful discussions regarding molecular diffusivity in catalysis. We also thank the Laboratory for Molecular Simulation (LMS) at Texas A&M University for providing software and computer time and Dr. Lisa M. Thomson, Manager of the LMS, for her assistance with the molecular modeling studies. Finally, we are particularly grateful to one of the reviewers of this article for pointing out an incorrect interpretation of two of the NMR spectra.

**Supporting Information Available:** TEM images and particle size distributions of the G4OH/Pd(0)40 catalysts prior to the hydrogenation reactions and <sup>1</sup>H NMR spectra of mixtures of 5 × 10<sup>-6</sup> M G4OH/Pd(0)40 and three allylic alcohols (**1**, **4**, and **5**) before and after exposure to H<sub>2</sub> (PDF). This material is available free of charge via the Internet at <http://pubs.acs.org>.

JA0105257

(39) Valden, M.; Lai, X.; Goodman, D. W. *Science* **1998**, *281*, 1647–1650.